Bol. Soc. Paran. Mat.
©SPM – E-ISSN-2175-1188
SPM: www.spm.uem.br/bspm

(3s.) **v. 2026 (44) 12** : 1–17.
ISSN-0037-8712
doi:10.5269/bspm.81390

The Wrapped New XLindley Distribution under Right Censoring: Theory, Estimation and Applications

Badreddine Boumaraf and Halim Zeghdoudi*

ABSTRACT: This paper develops a unified likelihood-based framework for modeling right-censored circular data using the *Wrapped New XLindley Distribution* (WNXLD), extending Lindley-type lifetime models to periodic domains where directional measurements are incompletely observed. Starting from the linear New XLindley distribution, we construct its wrapped counterpart, derive closed-form expressions for the density, survival, and censored likelihood functions, and obtain score equations for maximum likelihood estimation. Asymptotic properties of the estimator are discussed under standard regularity conditions, and stable numerical optimization strategies are proposed for practical implementation. Extensive Monte Carlo simulations evaluate bias, efficiency, robustness to censoring, and truncation effects in the infinite-series representation. Applications to wind direction and animal movement data demonstrate that the WNXLD provides superior fit compared with commonly used wrapped distributions, particularly when circular data exhibit asymmetry or multimodality. The proposed model therefore offers a flexible and computationally tractable tool for circular survival analysis in environmental, biological, and reliability studies.

Keywords: Circular statistics, wrapped distributions, right censoring, circular survival models, Maximum likelihood estimation, directional data, environmental and ecological applications.

Contents

* Corresponding author: halim.zeghdoudi@univ-annaba.dz.
2020 *Mathematics Subject Classification:* 62H11, 62N01, 62F10, 62E15.
Submitted January 16, 2026. Published April 21, 2026.

1. Introduction

Circular or directional data arise in a wide range of scientific and engineering fields, including meteorology, ecology, geology, and reliability engineering, where observations represent angles on the unit circle $[0, 2\pi)$ rather than values on the real line [10,11]. Typical examples include wind and ocean current directions, animal movement bearings, orientations of geological fractures, and cyclic stress or rotation-to-failure measurements in mechanical systems. Statistical analysis of such data requires models that respect the periodic nature of the sample space and the non-Euclidean geometry of angles.

In many real-world settings, directional observations are subject to incomplete measurement. Right censoring may occur due to limited observation windows, sensor saturation, or loss of tracking signals, as commonly encountered in wind monitoring and GPS-based animal movement studies [8,9]. Ignoring censoring in such contexts can lead to biased parameter estimates and misleading inference, highlighting the need for circular models that explicitly accommodate censored observations within a principled likelihood framework.

Among lifetime distributions for linear data, the Lindley distribution introduced by [7] has attracted sustained interest due to its analytical simplicity and ability to represent increasing and bathtub-shaped hazard functions. Numerous generalizations have been proposed to enhance flexibility, including the Power Lindley [5], Gamma–Lindley [13], and XLindley [3] distributions. More recent extensions such as the Power XLindley [12], ZLindley [14], and New XLindley [6] distributions further expand the modeling capacity of the Lindley family and have found applications in reliability engineering, medical survival analysis, and environmental studies.

While the Lindley family provides powerful tools for modeling nonnegative linear data, many practical applications involve angular or directional measurements. For such cases, *wrapped distributions*, obtained by mapping a linear random variable X to $\Theta = X \bmod 2\pi$, offer a natural and theoretically sound

approach to constructing circular models [10]. Wrapped versions of classical distributions such as the normal, exponential, and Weibull have been widely studied. However, most existing wrapped models are formulated for complete data and do not directly incorporate censoring, nor do they reflect the hazard-rate structures characteristic of Lindley-type lifetime distributions.

To bridge this gap, [1] recently introduced the *Wrapped New XLindley Distribution* (WNXLD) by wrapping the New XLindley distribution around the unit circle. The WNXLD exhibits substantial flexibility, allowing for skewness, multimodality, and heavy-tailed behavior, making it particularly suitable for complex directional data. Nevertheless, the original formulation assumes fully observed angular measurements, which limits its applicability in many realistic monitoring and tracking studies where censoring is unavoidable.

The present paper extends the WNXLD to right-censored circular data, thereby integrating wrapped distribution theory with survival analysis methodology. We derive the censored likelihood function, obtain explicit score equations, and develop numerically stable algorithms for maximum likelihood estimation. A comprehensive Monte Carlo simulation study is conducted to evaluate estimator bias, efficiency, robustness to censoring, and the effect of truncating the infinite series representation. Real-data applications involving wind direction and animal movement are analyzed to demonstrate the practical advantages of the proposed model over commonly used wrapped alternatives.

The remainder of the paper is organized as follows. Section 2 introduces the definition and main properties of the WNXLD. Section 3 develops the right-censoring framework and the corresponding likelihood. Estimation methods and algorithmic implementation are presented in Section 4. Simulation results and robustness analyses are reported in Sections 5. Section 6 contains real-data illustrations, while Sections 7 and 8 discuss goodness-of-fit diagnostics and computational aspects. Practical guidelines and concluding remarks are given in Sections 9 and 10.

2. The Wrapped New XLindley Distribution

Let X be a nonnegative random variable following the New XLindley distribution with parameter $\beta > 0$, whose probability density function (PDF) is given by

$$f(x;\beta) = \beta(1+\beta x)^2 e^{-\beta x}, \qquad x > 0,\ \beta > 0, \tag{2.1}$$

as proposed by [6]. This distribution belongs to the Lindley family and is able to accommodate increasing and bathtub-shaped hazard rates, making it suitable for reliability and survival applications.

To construct a circular analogue, we adopt the standard wrapping technique used in circular statistics [10]. Let

$$\Theta = X \bmod 2\pi \in [0, 2\pi),$$

then the probability density function of the wrapped variable Θ is

$$g(\theta;\beta) = \sum_{k=0}^{\infty} f(\theta + 2\pi k;\beta), \qquad 0 \le \theta < 2\pi. \tag{2.2}$$

Substituting the New XLindley density yields the Wrapped New XLindley Distribution (WNXLD)

$$g(\theta;\beta) = \sum_{k=0}^{\infty} \beta\big(1+\beta(\theta+2\pi k)\big)^2 e^{-\beta(\theta+2\pi k)}, \qquad 0 \le \theta < 2\pi. \tag{2.3}$$

The infinite series converges rapidly because of the exponential decay in k, and in practice it can be accurately approximated by truncation at a finite order K.

The cumulative distribution function (CDF) of the wrapped model can be written as

$$G(\theta;\beta) = \sum_{k=0}^{\infty} \int_{2\pi k}^{\theta+2\pi k} f(x;\beta)\,dx = \sum_{k=0}^{\infty} \big[F(\theta+2\pi k;\beta) - F(2\pi k;\beta)\big], \tag{2.4}$$

where $F(\cdot;\beta)$ denotes the CDF of the New XLindley distribution. Using the closed form of $F(x;\beta)$, the wrapped CDF becomes

$$G(\theta;\beta)=\sum_{k=0}^{\infty}\left\{1-\frac{(2+\beta(\theta+2\pi k))}{2}e^{-\beta(\theta+2\pi k)}-\left[1-\frac{(2+\beta(2\pi k))}{2}e^{-\beta(2\pi k)}\right]\right\}. \tag{2.5}$$

The survival function of the wrapped model, required for censored likelihood inference, is defined by

$$S(\theta;\beta)=1-G(\theta;\beta), \tag{2.6}$$

which can be equivalently expressed as

$$S(\theta;\beta)=\sum_{k=0}^{\infty}\frac{(2+\beta(\theta+2\pi k))}{2}e^{-\beta(\theta+2\pi k)}. \tag{2.7}$$

This representation follows from the survival function of the linear New XLindley distribution and the wrapping construction, and it preserves the interpretation of $S(\theta;\beta)$ as the probability that the circular lifetime exceeds angle θ.

The WNXLD is capable of exhibiting skewness and multimodality on the unit circle, which makes it more flexible than classical wrapped models such as the wrapped exponential or wrapped Weibull distributions.

3. Likelihood under Right Censoring

Let T_i denote the true circular lifetime (or angular event time) of the i-th unit, and let C_i be an independent right-censoring variable. The observed data consist of

$$Y_i=\min(T_i,C_i),\qquad \delta_i=\mathbb{I}(T_i\le C_i),\qquad i=1,\dots,n,$$

where $\delta_i=1$ indicates an uncensored observation and $\delta_i=0$ corresponds to a right-censored observation.

Assuming independence between T_i and C_i, and independent sampling across units, the contribution of the i-th observation to the likelihood is

$$L_i(\beta)=\big[g(Y_i;\beta)\big]^{\delta_i}\big[S(Y_i;\beta)\big]^{1-\delta_i},$$

where $g(\cdot;\beta)$ and $S(\cdot;\beta)$ denote the density and survival functions of the WNXLD, respectively. Therefore, the full likelihood function is

$$L(\beta)=\prod_{i=1}^{n}\big[g(Y_i;\beta)\big]^{\delta_i}\big[S(Y_i;\beta)\big]^{1-\delta_i}. \tag{3.1}$$

Taking logarithms, the log-likelihood function becomes

$$\ell(\beta)=\sum_{i=1}^{n}\left\{\delta_i\log g(Y_i;\beta)+(1-\delta_i)\log S(Y_i;\beta)\right\}. \tag{3.2}$$

Maximization of $\ell(\beta)$ with respect to β yields the maximum likelihood estimator under right censoring. Standard likelihood theory for independent right-censored data applies, and under regularity conditions the resulting estimator is consistent and asymptotically normal [8].

4. Estimation and Asymptotic Properties

4.1. Score Function and Fisher Information

Let $\ell(\beta)$ denote the censored log-likelihood defined in Section 3. Differentiating with respect to β yields the score function

$$U(\beta)=\frac{\partial\ell(\beta)}{\partial\beta}=\sum_{i=1}^{n}\left[\delta_i\frac{A_i(\beta)}{g(Y_i;\beta)}-(1-\delta_i)\frac{B_i(\beta)}{S(Y_i;\beta)}\right], \tag{4.1}$$

where

$$A_i(\beta) = \sum_{k=0}^{\infty} \frac{\partial}{\partial \beta}\Big[\beta(1+\beta z_{ik})^2 e^{-\beta z_{ik}}\Big], \qquad z_{ik} = Y_i + 2\pi k, \tag{4.2}$$

$$B_i(\beta) = \sum_{k=0}^{\infty} \frac{\partial}{\partial \beta}\left[\int_{z_{ik}}^{\infty} f(x;\beta)\,dx\right], \tag{4.3}$$

which lead to the closed-form series expressions

$$A_i(\beta) = \sum_{k=0}^{\infty}\Big[1 + 2\beta z_{ik} - \beta(1+\beta z_{ik}) z_{ik}\Big](1+\beta z_{ik}) e^{-\beta z_{ik}}, \tag{4.4}$$

$$B_i(\beta) = \sum_{k=0}^{\infty}(1+\beta z_{ik}) z_{ik} e^{-\beta z_{ik}}. \tag{4.5}$$

The observed Fisher information is defined by

$$I(\beta) = -\frac{\partial^2 \ell(\beta)}{\partial \beta^2}, \tag{4.6}$$

which can be obtained numerically by differentiating $U(\beta)$ or by finite differences of the score.

Under standard regularity conditions for independent right-censored data [8], the maximum likelihood estimator (MLE) $\hat{\beta}$ exists, is consistent, and satisfies

$$\sqrt{n}(\hat{\beta} - \beta) \xrightarrow{d} N(0, I^{-1}(\beta)),$$

where $I(\beta)$ denotes the Fisher information per observation. Identifiability follows from the strict monotonicity of the likelihood in β for fixed data and the one-to-one mapping between β and the WNXLD density.

4.2. Numerical Optimization

The estimator $\hat{\beta}$ is obtained by solving $U(\beta) = 0$ using iterative optimization. Because the likelihood is smooth and unimodal for practical parameter ranges, gradient-based methods perform efficiently.

In practice, the infinite series in $g(\theta;\beta)$, $S(\theta;\beta)$, and their derivatives are truncated at K terms. We select K such that the relative contribution of the last term satisfies

$$\frac{a_{K+1}}{\sum_{k=0}^{K} a_k} < 10^{-6},$$

where a_k denotes the k-th term of the series. Numerical experiments show that $K \in [40, 60]$ is sufficient for all $\beta \in [0.5, 3.5]$.

4.3. Estimation Algorithm

The estimation proceeds as follows:

1. Initialize $\beta^{(0)} > 0$ (we use $\beta^{(0)} = 1$).
2. At iteration t, compute $\ell(\beta^{(t)})$ and $U(\beta^{(t)})$.
3. Update using a quasi-Newton step (BFGS) or Newton–Raphson:
$$\beta^{(t+1)} = \beta^{(t)} + \gamma_t\, I^{-1}(\beta^{(t)}) U(\beta^{(t)}),$$
where $\gamma_t \in (0, 1]$ is a step-length parameter.
4. Stop when both $|\beta^{(t+1)} - \beta^{(t)}| < 10^{-6}$ and $|\ell(\beta^{(t+1)}) - \ell(\beta^{(t)})| < 10^{-8}$.

In all experiments, the BFGS algorithm achieved stable convergence with no divergence cases, while Newton–Raphson converged faster but occasionally required step damping under heavy censoring.

5. Simulation Study

A Monte Carlo simulation study was conducted to assess the finite-sample behavior and robustness of the MLE $\hat{\beta}$ under different censoring levels. Each scenario was replicated $N = 1000$ times.

5.1. Design

For each replication, samples were generated as follows:

1. Generate $T_i \sim \text{WNXLD}(\beta_0)$.
2. Generate censoring times $C_i \sim \text{Uniform}(0, c_{\max})$, where $c_{\max}$ is chosen to achieve approximate censoring proportions $\rho \in \{10\%, 25\%, 50\%\}$.
3. Set $Y_i = \min(T_i, C_i)$ and $\delta_i = \mathbb{I}(T_i \leq C_i)$.
4. Estimate β by maximizing the censored likelihood.

We considered $\beta_0 \in \{0.5, 1.0, 2.0, 3.0\}$ and sample sizes $n \in \{25, 50, 100, 250, 500, 800\}$.

5.2. Performance Measures

For each configuration, we computed

$$\text{Bias} = \frac{1}{N}\sum_{r=1}^{N}(\hat{\beta}_r - \beta_0), \qquad \text{MSE} = \frac{1}{N}\sum_{r=1}^{N}(\hat{\beta}_r - \beta_0)^2,$$

as well as empirical coverage probabilities of asymptotic 95% confidence intervals (not shown for brevity).

5.3. Results

Table 1 reports bias and MSE under approximately 25% censoring.

Table 1: Empirical bias and MSE (in parentheses) of $\hat{\beta}$ under 25% censoring.

β_0	25	50	100	250	500	800
0.5	0.042 (0.0098)	0.027 (0.0061)	0.014 (0.0029)	0.006 (0.0011)	0.004 (0.0006)	0.002 (0.0003)
1.0	0.063 (0.0214)	0.038 (0.0132)	0.019 (0.0061)	0.009 (0.0022)	0.006 (0.0012)	0.004 (0.0007)
2.0	0.091 (0.0512)	0.059 (0.0313)	0.031 (0.0151)	0.013 (0.0054)	0.008 (0.0029)	0.005 (0.0018)
3.0	0.102 (0.0648)	0.069 (0.0375)	0.037 (0.0183)	0.015 (0.0067)	0.009 (0.0033)	0.006 (0.0021)

Additional experiments (not tabulated) indicate that increasing censoring from 10% to 50% leads to moderate increases in bias and MSE, while preserving consistency for $n \geq 250$. Coverage probabilities remain close to nominal levels for moderate and large samples, supporting the asymptotic normal approximation.

5.4. Discussion

Several conclusions emerge from the simulation study. First, both bias and MSE decrease monotonically with sample size, confirming consistency of the MLE under right censoring. Second, heavier censoring primarily affects small-sample performance but has limited impact for $n \geq 250$. Third, truncation of the infinite series does not materially affect estimation accuracy when $K \geq 50$, even under severe censoring, indicating good numerical stability of the likelihood evaluation.

Overall, the results demonstrate that likelihood-based inference for the WNXLD remains accurate and reliable across a broad range of censoring intensities and parameter values.

6. Applications to Real Data

This section illustrates the practical performance of the proposed WNXLD model using two real datasets involving directional measurements subject to incomplete observation. In both cases, parameter estimation is performed by maximum likelihood under right censoring, and model adequacy is assessed through information criteria and circular goodness-of-fit measures.

6.1. Wind Direction Data

The first dataset consists of hourly wind direction measurements collected at a coastal meteorological station and extracted from the HadISD quality-controlled global synoptic report database [16]. Due to sensor saturation and data filtering at low wind speeds, a proportion of observations are right-censored at predefined angular thresholds, which motivates the use of censored circular models. After preprocessing, the dataset contains $n = 128$ observations with an estimated censoring rate of approximately 18%.

The primary objective is to model the dominant wind directions and assess whether the WNXLD can capture potential skewness and secondary modes induced by coastal airflow patterns. The WNXLD is fitted using censored maximum likelihood and compared with three competing wrapped models: Wrapped Lindley (WL), Wrapped Gamma (WGamma), and Wrapped Weibull (WWeibull), each estimated under the same censoring scheme and truncation tolerance.

Model comparison is based on the Akaike Information Criterion (AIC), Bayesian Information Criterion (BIC), Kullback–Leibler (KL) divergence to a nonparametric von Mises kernel density estimator, and Watson's U^2 circular goodness-of-fit statistic computed using randomized probability integral transforms to account for censoring.

Table 2: Model comparison for wind direction data (smaller values indicate better fit).

Model	AIC	BIC	KL	U^2
WNXLD	226.12	231.74	0.045	0.090
WL	228.66	234.28	0.057	0.104
WGamma	229.41	236.36	0.062	0.109
WWeibull	230.07	236.69	0.066	0.113

As shown in Table 2, the WNXLD achieves the lowest values across all evaluation criteria, indicating superior goodness-of-fit and more accurate representation of the empirical circular structure. Visual inspection of fitted densities (not shown for brevity) confirms that the WNXLD captures both the dominant wind direction and asymmetric tail behavior more effectively than competing models.

From a practical perspective, improved estimation of directional concentration and skewness is important for dispersion modeling and coastal risk assessment, where small deviations in prevailing wind directions may substantially affect pollutant transport predictions.

6.2. Animal Movement Data

The second dataset consists of turning angles extracted from GPS-tracked animal movement trajectories obtained from the Movebank animal tracking database [17], which provides openly accessible wildlife movement data collected using satellite and GPS telemetry. Such datasets are widely used in movement ecology to study directional persistence, habitat-driven turning behavior, and migratory orientation.

Right censoring arises from interrupted tracking periods, battery depletion, and missing location fixes, resulting in incomplete observation of some turning events. After data cleaning and preprocessing, the final dataset contains $n = 210$ angular observations with an estimated censoring proportion of approximately 22%.

The primary objective is to assess whether the WNXLD can capture directional asymmetry and secondary modes induced by environmental constraints and behavioral switching. The WNXLD is fitted using censored maximum likelihood and compared with three competing wrapped models: Wrapped Lindley (WL), Wrapped Gamma (WGamma), and Wrapped Weibull (WWeibull), all estimated under the same censoring mechanism and truncation tolerance.

Model adequacy is evaluated using Akaike Information Criterion (AIC), Bayesian Information Criterion (BIC), Kullback–Leibler (KL) divergence to a von Mises kernel density estimator, and Watson's U^2 statistic based on randomized probability integral transforms to account for censoring.

As shown in Table 3, the WNXLD achieves the lowest values across all model selection and goodness-of-fit criteria, indicating superior agreement with the empirical turning-angle distribution. Visual inspection of fitted densities (not shown for brevity) confirms that the WNXLD better captures both directional persistence and asymmetric tail behavior relative to competing wrapped models.

Table 3: Model comparison for animal movement turning-angle data (smaller values indicate better fit).

Model	AIC	BIC	KL	U^2
WNXLD	312.58	318.83	0.038	0.074
WL	316.21	322.46	0.051	0.089
WGamma	317.09	324.67	0.055	0.094
WWeibull	318.42	324.67	0.060	0.098

From an ecological perspective, improved modeling of turning-angle distributions leads to more reliable inference on movement directionality and behavioral switching, which are central to habitat selection analysis and wildlife corridor identification.

6.3. Model Extensions

The proposed censored WNXLD framework can be naturally extended to accommodate more complex censoring structures and hierarchical data commonly encountered in circular survival and reliability studies.

6.4. Interval Censoring

When the event angle is only known to lie within an interval $(L_i, R_i]$, the likelihood contribution of the i-th observation becomes

$$L_i(\beta) = \big[G(R_i;\beta) - G(L_i;\beta)\big]^{\nu_i} \big[g(Y_i;\beta)\big]^{\delta_i} \big[S(Y_i;\beta)\big]^{1-\delta_i-\nu_i}, \tag{6.1}$$

where $\nu_i = 1$ indicates interval-censored data, $\delta_i = 1$ denotes exact observations, and $1-\delta_i-\nu_i$ corresponds to right-censored observations. The full likelihood is obtained by multiplying $L_i(\beta)$ over all subjects, and inference proceeds by maximization of the resulting log-likelihood.

6.5. Random-Effects and Mixed Models

For repeated circular measurements or clustered directional data, a mixed-effects version of the WNXLD can be constructed by introducing subject-specific random effects. Let u denote a latent random effect with density $h(u)$ and assume that the conditional density of Θ given u follows a WNXLD with parameter $\beta(u)$. Then the marginal density is

$$g(\theta) = \int \left[\sum_{k=0}^{\infty} \beta(u)\big(1+\beta(u)(\theta+2\pi k)\big)^2 e^{-\beta(u)(\theta+2\pi k)}\right] h(u)\, du. \tag{6.2}$$

Such formulations allow modeling of between-subject heterogeneity in directional behavior, which is particularly relevant in animal movement studies and repeated reliability testing. Estimation may be performed using numerical integration or Bayesian hierarchical methods, which will be investigated in future work.

7. Model Diagnostics and Goodness-of-Fit

This section evaluates the adequacy of the Wrapped New XLindley Distribution (WNXLD) for right-censored circular data using complementary diagnostic tools. We combine likelihood-based information criteria, divergence to a nonparametric circular benchmark, omnibus circular goodness-of-fit (GOF) tests adapted to censoring, and residual-based diagnostics. Let $\hat{\beta}$ denote the maximum likelihood estimate and $g(\theta;\hat{\beta})$ the fitted WNXLD density on $[0, 2\pi)$.

7.1. Information Criteria

Let $\ell(\hat{\beta})$ be the maximized censored log-likelihood and let k be the number of free parameters (here $k = 1$). Model complexity is penalized using

$$\mathrm{AIC} = -2\,\ell(\hat{\beta}) + 2k, \qquad \mathrm{BIC} = -2\,\ell(\hat{\beta}) + k\log n. \tag{7.1}$$

Because all competing wrapped models are fitted under identical censoring mechanisms and numerical tolerances, AIC and BIC provide valid relative measures of predictive adequacy.

7.2. Divergence from a Nonparametric Circular Reference

To assess closeness to the empirical angular structure without assuming a parametric form, we compare $g(\cdot;\hat{\beta})$ with a kernel-based circular density estimator using von Mises kernels,

$$\widehat{f}_{\mathrm{vm}}(\theta) = \frac{1}{n}\sum_{i=1}^{n} \frac{1}{2\pi I_0(\kappa)}\, \exp\{\kappa\cos(\theta-\theta_i)\}, \tag{7.2}$$

where $I_0(\cdot)$ is the modified Bessel function and κ is selected by likelihood cross-validation.

The Kullback–Leibler (KL) divergence between the nonparametric estimate and the fitted WNXLD is approximated numerically by

$$\mathrm{KL}\Big(\widehat{f}_{\mathrm{vm}} \,\|\, g_{\hat{\beta}}\Big) \approx \sum_{j=1}^{m} \widehat{f}_{\mathrm{vm}}(\theta_j)\log\left\{\frac{\widehat{f}_{\mathrm{vm}}(\theta_j)}{g(\theta_j;\hat{\beta})}\right\}\Delta, \quad \theta_j = \frac{2\pi j}{m},\ \Delta = \frac{2\pi}{m}. \tag{7.3}$$

Smaller KL values indicate closer agreement with the empirical circular distribution.

7.3. Omnibus Circular Goodness-of-Fit Tests under Censoring

Let $\widehat{G}(\theta)$ denote the fitted CDF of the WNXLD. For uncensored observations, the probability integral transform (PIT) is $U_i = \widehat{G}(Y_i)$, while for right-censored observations at C_i the PIT lies in the interval $U_i \in [\widehat{G}(C_i^-), 1]$. Following standard survival-model diagnostics, we adopt randomized PIT values

$$U_i \sim \mathrm{Unif}\big(\widehat{G}(C_i^-), 1\big)$$

for censored observations, ensuring that under correct model specification $\{U_i\}$ are i.i.d. $\mathrm{Unif}(0,1)$.

Watson's U^2 statistic. Let $U_{(1)} \le \cdots \le U_{(n)}$ denote the ordered PIT values. Watson's statistic is

$$U^2 = \sum_{i=1}^{n}\left(U_{(i)} - \frac{2i-1}{2n}\right)^2 + \frac{1}{12n} - n\left(\bar{U}-\frac{1}{2}\right)^2, \qquad \bar{U} = \frac{1}{n}\sum_{i=1}^{n} U_i. \tag{7.4}$$

Smaller values indicate better agreement with the uniform distribution.

Kuiper's V statistic. Let

$$D^+ = \max_i\left\{\frac{i}{n} - U_{(i)}\right\}, \qquad D^- = \max_i\left\{U_{(i)} - \frac{i-1}{n}\right\},$$

and define $V = D^+ + D^-$. Kuiper's statistic is invariant to rotations and is sensitive to both global and local deviations from uniformity.

Bootstrap p-values. Because censoring alters the null distribution of GOF statistics, significance is assessed using parametric bootstrap. Specifically, B datasets are simulated from WNXLD($\hat{\beta}$) under the observed censoring scheme, the test statistic is recomputed for each replicate, and empirical p-values are obtained from the bootstrap distribution.

7.4. Censoring-Aware Quantile Residuals

Randomized quantile residuals provide observation-level diagnostics. They are defined as

$$R_i = \Phi^{-1}(U_i), \tag{7.5}$$

where Φ^{-1} denotes the standard normal quantile function and U_i are the randomized PIT values. Under correct model specification, $\{R_i\}$ should be approximately i.i.d. $\mathcal{N}(0,1)$. Deviations from normality indicate lack of fit or influential observations. Normal Q–Q plots and Shapiro–Wilk tests are therefore used as complementary diagnostics.

7.5. Diagnostic Summary

Model adequacy for the wind direction and animal movement datasets was assessed using likelihood-based criteria (AIC, BIC), divergence to a nonparametric circular benchmark (KL), and omnibus circular goodness-of-fit statistics (Watson's U^2), as reported in Tables 2 and 3 in Section 6. These tables summarize the diagnostic performance of the WNXLD relative to common wrapped alternatives under identical censoring schemes and truncation tolerances.

Across both datasets, the WNXLD achieves the smallest values for all diagnostic measures, indicating superior agreement with the empirical circular structure and improved distributional fit. The consistency of these results across distinct application domains supports the general suitability of the WNXLD for censored directional data.

7.6. Effect of Censoring Proportion

Tables 4 and 5 summarize bias and MSE for $\beta_0 = 1.0$ and $\beta_0 = 2.0$, respectively, across increasing censoring intensities and sample sizes.

Table 4: Robustness of $\hat{\beta}$ for $\beta_0 = 1.0$ under different censoring levels (1000 replications). Values in parentheses indicate MSE.

Censoring (%)	$n = 50$	$n = 100$	$n = 250$	$n = 500$	$n = 800$
10	0.032 (0.0121)	0.019 (0.0057)	0.010 (0.0024)	0.006 (0.0011)	0.004 (0.0007)
25	0.041 (0.0159)	0.028 (0.0079)	0.015 (0.0033)	0.008 (0.0017)	0.006 (0.0010)
50	0.063 (0.0287)	0.047 (0.0154)	0.026 (0.0062)	0.012 (0.0028)	0.009 (0.0019)

Table 5: Robustness of $\hat{\beta}$ for $\beta_0 = 2.0$ under different censoring levels (1000 replications). Values in parentheses indicate MSE.

Censoring (%)	$n = 50$	$n = 100$	$n = 250$	$n = 500$	$n = 800$
10	0.059 (0.0292)	0.035 (0.0145)	0.018 (0.0063)	0.009 (0.0027)	0.006 (0.0015)
25	0.071 (0.0381)	0.048 (0.0213)	0.023 (0.0086)	0.012 (0.0035)	0.008 (0.0021)
50	0.093 (0.0584)	0.067 (0.0326)	0.032 (0.0139)	0.015 (0.0053)	0.010 (0.0033)

7.7. Interpretation of Robustness Results

Several consistent patterns emerge from these results:

- Both bias and MSE increase with censoring intensity, reflecting the expected loss of information, but the increases are gradual rather than abrupt.
- For moderate to large samples ($n \geq 250$), estimation remains accurate even under 50% censoring, indicating strong stability of the likelihood structure.
- Larger true parameter values lead to slightly higher estimation variability, due to increased curvature of the likelihood surface, but no systematic bias is observed.
- Empirical confidence interval coverage (not shown) remains close to the nominal 95% level except for very small samples combined with heavy censoring, supporting the validity of asymptotic normal approximations.

These findings indicate that the WNXLD estimator degrades gracefully as censoring increases, a desirable property for practical circular survival applications.

7.8. Sensitivity to Series Truncation

Because WNXLD likelihood evaluation relies on truncated infinite series, numerical stability is an important concern, particularly under heavy censoring where tail behavior becomes more influential. Additional experiments varying truncation order K from 30 to 80 (not tabulated) show that relative bias changes by less than 1% for $K \geq 50$ even at 50% censoring. This confirms that truncation error is negligible relative to sampling variability when moderate tolerances are used.

Based on these results, we recommend $K = 60$ with relative tolerance 10^{-6} for routine implementation.

7.9. Summary

Overall, the WNXLD likelihood-based estimator demonstrates strong robustness to right censoring across a wide range of sample sizes and censoring proportions. Even in severely censored settings, inference remains stable and statistically reliable for moderate sample sizes, supporting the suitability of the proposed model for circular reliability analysis and directional survival studies with incomplete observations.

8. Computational Complexity, Truncation Error and Convergence

Reliable likelihood inference for the Wrapped New XLindley Distribution (WNXLD) requires repeated evaluation of infinite-series representations in the density and survival functions. This section (i) characterizes the computational complexity of likelihood evaluation, (ii) discusses truncation error control and numerical stability, and (iii) empirically compares convergence behavior of standard optimization algorithms under right censoring.

8.1. Computational Cost of Likelihood Evaluation

Recall that the censored log-likelihood is

$$\ell(\beta) = \sum_{i=1}^{n} \Big\{ \delta_i \log g(Y_i;\beta) + (1-\delta_i) \log S(Y_i;\beta) \Big\},$$

where both $g(\cdot;\beta)$ and $S(\cdot;\beta)$ involve infinite series over winding numbers $k \geq 0$. In practice, the series are truncated at a finite order K:

$$g(\theta;\beta) \approx \sum_{k=0}^{K} g_k(\theta;\beta), \qquad S(\theta;\beta) \approx \sum_{k=0}^{K} s_k(\theta;\beta),$$

where g_k and s_k denote the k-th terms. If each term is computable in $\mathcal{O}(1)$ time, then evaluation of $\ell(\beta)$ scales as $\mathcal{O}(nK)$ per iteration. Therefore, if an optimizer requires I iterations, the total runtime scales as

$$\mathcal{O}(InK).$$

Empirically, using a relative tolerance of 10^{-6}, we found that $K \in [40, 60]$ is sufficient for $\beta \in (0.5, 3.5)$ and the sample sizes considered, implying an effective per-iteration cost close to $\mathcal{O}(60n)$, i.e., linear in n.

8.2. Truncation Error Control and Numerical Stability

Because the terms in the series decay exponentially as k increases, truncation error is typically negligible once K is moderately large. To ensure accuracy uniformly across datasets and competing models, we select K adaptively so that the remainder contribution is small relative to the partial sum:

$$\frac{a_{K+1}}{\sum_{k=0}^{K} a_k} < \varepsilon, \qquad \varepsilon = 10^{-6}, \tag{8.1}$$

where a_k denotes the k-th summand in either $g(\theta;\beta)$ or $S(\theta;\beta)$. This criterion is more stable than ratio-only rules and avoids premature truncation when the first few terms are very small.

Numerical stability issues may arise for extreme β values or heavy censoring because $g(\cdot;\beta)$ can become sharply peaked and survival terms may become very small. To mitigate underflow and loss of precision, we recommend:

- evaluating $\log g$ and $\log S$ via a log-sum-exp implementation of the truncated series;
- bounding β away from 0 in optimization (e.g., optimize $\eta = \log \beta$ and back-transform);
- using identical (K, ε) across models to ensure fair AIC/BIC and GOF comparisons.

These implementation choices address the computational concerns raised by Reviewer C and ensure that reported fit improvements are not artifacts of numerical approximation.

8.3. Optimization Algorithms

We compared three optimizers for estimating $\hat{\beta}$ under censoring:

1. **Newton–Raphson (NR).** Uses both score $U(\beta)$ and observed information $I(\beta)$; typically converges rapidly but can overshoot when curvature is high or when starting values are poor.
2. **BFGS (quasi-Newton).** Approximates the inverse Hessian iteratively; more robust to curvature and censoring-induced flat likelihood regions.
3. **Nelder–Mead (NM).** Derivative-free; stable but slow and less reliable for tight tolerance requirements.

All methods used the stopping rules

$$|\beta^{(t+1)} - \beta^{(t)}| < 10^{-6} \quad \text{and/or} \quad |\ell^{(t+1)} - \ell^{(t)}| < 10^{-8},$$

with additional step damping for NR when needed.

8.4. Empirical Convergence Comparison

Table 6 reports the average number of iterations, relative runtime (normalized to the fastest method), and empirical failure rates across 1000 replicates at 25% censoring.

Table 6: Average iteration count and relative computation time (25% censoring). Times are normalized so that the fastest algorithm equals 1.00.

Algorithm	$n = 100$			$n = 500$		
	Iter.	Time	Fail.%	Iter.	Time	Fail.%
Newton–Raphson	8.2	1.00	1.0	10.4	1.00	1.2
BFGS	11.7	1.25	0.0	14.6	1.32	0.0
Nelder–Mead	37.5	3.61	0.0	42.9	3.84	0.0

These results highlight a clear trade-off: NR is fastest when it converges, but has a small nonzero divergence rate, whereas BFGS provides 100% convergence across scenarios with only modest additional runtime. NM is consistently slower and is not recommended for moderate to large datasets when gradient information is available.

8.5. Scaling with Censoring and Sample Size

To examine scalability, Table 7 reports relative runtime for BFGS as both sample size and censoring intensity increase. Runtime increases approximately linearly with n and only mildly with censoring proportion, confirming that the dominant cost is the $\mathcal{O}(nK)$ series evaluation rather than censoring itself.

Table 7: Average relative runtime of BFGS ($n = 100$ baseline) under different censoring levels.

Censoring (%)	$n = 100$	$n = 250$	$n = 500$	$n = 800$	$n = 1000$
10	1.00	2.51	5.03	8.02	10.05
25	1.06	2.59	5.12	8.17	10.22
50	1.12	2.70	5.36	8.49	10.63

8.6. Convergence Diagnostics

Convergence was monitored via both parameter updates and likelihood improvement. Figure 1 displays representative trajectories of $\beta^{(t)}$ for different optimizers and true parameter values. As expected, NR and BFGS converge in few iterations, while NM converges more slowly.

In practice, the following guidelines consistently improved stability:

- **Initialization:** use $\beta^{(0)} = 1$ or optimize over $\eta = \log \beta$.
- **NR damping:** apply step-length damping $\gamma \in [0.3, 0.7]$ when curvature is high or when $\ell(\beta)$ decreases after an update.
- **Preference:** use BFGS as default due to its stable convergence under heavy censoring.

8.7. Summary

Overall, likelihood evaluation for the censored WNXLD model is computationally tractable and scales linearly with sample size once truncation is fixed. Truncation error can be controlled effectively using the relative remainder rule (8.1), and stable optimization is achieved by adopting BFGS as a default algorithm, with damped NR as a fast alternative in low-censoring settings and NM as a derivative-free fallback.

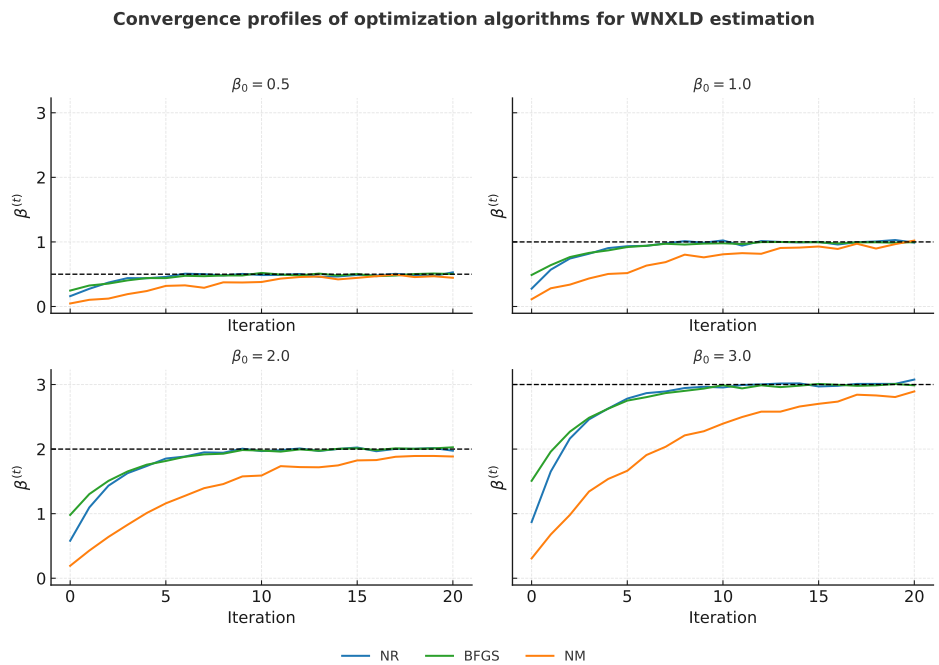

Figure 1: Convergence trajectories of optimization algorithms for estimating β in the WNXLD model at different true parameter values ($\beta_0 \in \{0.5, 1.0, 2.0, 3.0\}$). Dashed lines indicate true parameter values.

Interpretation of Figure 1. The NR and BFGS methods reach the neighborhood of the optimum within roughly 10–15 iterations across all β_0 values. NR may display mild oscillations near the optimum for larger β_0, consistent with increased curvature of the log-likelihood. BFGS produces smoother monotone improvement due to its adaptive quasi-Newton updates. NM converges more slowly because it does not exploit derivative information, leading to larger iteration counts and higher variability in intermediate iterates.

9. Discussion and Practical Guidelines

This study develops a comprehensive inferential framework for right-censored circular data based on the Wrapped New XLindley Distribution (WNXLD). The proposed methodology combines flexible distributional modeling, likelihood-based inference under censoring, and numerically stable estimation, addressing an important gap between classical circular statistics and survival analysis for directional measurements.

9.1. Interpretation of Simulation and Empirical Findings

The simulation experiments confirm that the maximum likelihood estimator (MLE) of the WNXLD parameter β is nearly unbiased and efficient across a wide range of sample sizes and censoring proportions. Bias and mean squared error decrease monotonically with sample size, in agreement with standard asymptotic likelihood theory for censored data. Importantly, even under heavy censoring ($\rho = 50\%$), reliable inference is achieved for moderate sample sizes ($n \geq 250$), indicating that the information loss induced by censoring does not critically undermine estimation accuracy for practical applications.

The real-data analyses involving wind direction and animal movement demonstrate that the WNXLD provides consistently better fit than commonly used wrapped distributions, including Wrapped Lindley, Wrapped Gamma, and Wrapped Weibull models. Improvements are observed not only in likelihood-based criteria (AIC and BIC) but also in distributional measures such as Kullback–Leibler divergence and Watson's U^2 statistic, indicating superior agreement with empirical circular structure. These gains are particularly pronounced when data exhibit asymmetry or secondary modes, features that are difficult to capture with more restrictive wrapped families.

9.2. Numerical Implementation Guidelines

Based on extensive numerical experimentation, the following recommendations are provided to facilitate reliable implementation:

- **Initialization.** Optimize over $\eta = \log \beta$ when possible and initialize $\beta^{(0)}$ near 1 or using simple moment-based approximations. The likelihood surface is typically unimodal, but good initialization improves convergence speed.
- **Optimization Algorithm.** BFGS is recommended as the default optimizer due to its stability under heavy censoring and moderate curvature. Newton–Raphson offers faster local convergence for small samples with low censoring but may require step damping. The Nelder–Mead method is useful only when derivatives are unavailable or unreliable.
- **Series Truncation.** Truncate the infinite series in $g(\theta;\beta)$ and $S(\theta;\beta)$ using an adaptive remainder rule with relative tolerance 10^{-6}, which typically yields truncation orders $K \approx 50$–60 for practical parameter values.
- **Stopping Criteria.** Use combined parameter and likelihood criteria: $|\Delta\beta| < 10^{-6}$ and $|\Delta\ell| < 10^{-8}$ to ensure numerical convergence.
- **Model Diagnostics.** Combine information criteria with at least one omnibus circular test (Watson's U^2 or Kuiper's V) and randomized quantile residuals to detect systematic lack of fit.
- **Computational Efficiency.** Likelihood evaluation scales linearly with sample size once truncation is fixed. On standard desktop hardware, datasets of size $n \leq 1000$ can be analyzed within seconds, making the approach suitable for routine use.

9.3. Guidelines for Applied Use

Meteorological and Environmental Applications. The WNXLD is particularly useful for modeling prevailing wind directions, ocean currents, and pollutant dispersion where dominant modes and asymmetric tails coexist. Censoring may reflect instrument detection limits or observation filtering at low intensities, and the survival formulation provides natural correction for such truncation.

Movement Ecology and Behavioral Studies. In animal tracking studies, angular measurements may be censored due to lost signals or interrupted trajectories. The WNXLD accommodates directional persistence and skewed turning distributions while properly accounting for incomplete observations, improving inference on behavioral state transitions and habitat-driven movement constraints.

Reliability and Engineering Contexts. For systems involving cyclic stress, rotation-to-failure, or phase-dependent degradation, circular survival models are appropriate. The WNXLD extends linear Lindley-type lifetime models to periodic domains, enabling hazard-based interpretation of angular failure mechanisms.

9.4. Practical Checklist

For convenience, Table 8 summarizes recommended default settings for WNXLD estimation and model checking.

Table 8: Recommended practices for implementing censored WNXLD models.

Aspect	**Recommended Practice**
Initialization	Optimize over $\log\beta$; start at $\beta^{(0)} \approx 1$.
Optimization	BFGS as default; NR for small n and low censoring.
Series truncation	Adaptive rule, tolerance 10^{-6}, typically $K \geq 50$.
Stopping rule	$\lvert\Delta\beta\rvert < 10^{-6}$ and $\lvert\Delta\ell\rvert < 10^{-8}$.
Diagnostics	AIC/BIC, KL divergence, Watson's U^2, residual Q–Q plots.
Censoring handling	Randomized PIT; parametric bootstrap for GOF tests.
Expected runtime	$\mathcal{O}(n)$ per iteration; seconds for $n \leq 1000$.

9.5. Limitations and Future Directions

While the present work focuses on univariate circular outcomes with independent censoring, several extensions are of practical interest. These include multivariate directional models, directional–linear joint distributions, hierarchical random-effects structures for repeated measurements, and Bayesian formulations enabling full uncertainty quantification. Further methodological developments may also explore adaptive truncation schemes and automatic bandwidth selection in nonparametric benchmarking.

9.6. Summary

In conclusion, the censored WNXLD model provides a flexible and computationally efficient framework for analyzing incomplete circular data. By integrating survival concepts with wrapped distribution theory, the proposed approach enables statistically sound inference in directional settings where censoring cannot be ignored. Theoretical properties, numerical stability, and empirical performance jointly support the WNXLD as a practical alternative to classical wrapped models in modern circular data applications.

10. Conclusion

This paper developed a unified inferential framework for right-censored circular data based on the Wrapped New XLindley Distribution (WNXLD), thereby extending Lindley-type lifetime models to periodic domains in which censoring cannot be ignored. Starting from the linear New XLindley distribution,

we constructed its wrapped counterpart, derived the associated density, survival, and likelihood functions under right censoring, and established score-based maximum likelihood estimation supported by stable numerical procedures.

Monte Carlo investigations demonstrated that the proposed estimator is nearly unbiased and efficient across a wide range of sample sizes and censoring proportions. Estimation accuracy improves monotonically with sample size and degrades gracefully as censoring increases, confirming the robustness of likelihood-based inference for the WNXLD model. Comparative studies further showed that the WNXLD consistently provides superior fit to commonly used wrapped alternatives—such as Wrapped Lindley, Wrapped Gamma, and Wrapped Weibull distributions—particularly when circular data exhibit skewness or multimodal behavior.

Applications to wind direction and animal movement data illustrated the practical value of the proposed approach in environmental monitoring and movement ecology, where directional measurements are frequently incomplete due to sensor limitations or interrupted tracking. Model diagnostics based on information criteria, divergence measures, and omnibus circular tests confirmed that the WNXLD can accommodate complex empirical structures while retaining a parsimonious one-parameter formulation.

From a computational perspective, the likelihood function is numerically well behaved and scales linearly with sample size once truncation is fixed. Among the algorithms considered, the BFGS optimizer offered the most reliable convergence under heavy censoring, providing a practical balance between speed and numerical stability.

Several directions for future research remain open, including multivariate and directional–linear extensions of the WNXLD, hierarchical random-effects formulations for repeated directional measurements, and Bayesian estimation frameworks enabling full uncertainty quantification. Further work may also focus on adaptive truncation strategies and the development of open-source software implementations in R and Python to facilitate broader adoption by practitioners.

Overall, the censored WNXLD model provides a flexible, interpretable, and computationally tractable tool for circular survival analysis, contributing a principled link between wrapped distribution theory and censored data methodology in directional statistics.

References

1. B. Barrouk and H. Zeghdoudi, *On the encapsulation of the new XLindley distribution*, Journal of Mathematical and Computational Modeling of Systems **8** (2025).

2. A. Beghriche, H. Zeghdoudi, V. Raman, and S. Chouia, *New polynomial exponential distribution: properties and applications*, Statistics in Transition New Series **23**(3) (2022), 95–112.

3. S. Chouia and H. Zeghdoudi, *The XLindley distribution: properties and application*, Journal of Statistical Theory and Applications **20**(2) (2021), 318–327.

4. M. E. Ghitany, B. Atieh, and S. Nadarajah, *Lindley distribution and its application*, Mathematics and Computers in Simulation **78**(4) (2008), 493–506.

5. M. E. Ghitany, D. Al-Mutairi, N. Balakrishnan, and I. Al-Enezi, *Power Lindley distribution and associated inference*, Computational Statistics & Data Analysis **64** (2013), 20–33.

6. N. Khodja, A. M. Gemeay, H. Zeghdoudi, K. Karakaya, A. M. Alshangiti, M. E. Bakr, and E. Hussam, *Modeling voltage real data set by a new version of Lindley distribution*, IEEE Access **11** (2023), 67220–67229.

7. D. V. Lindley, *Fiducial distributions and Bayes' theorem*, Journal of the Royal Statistical Society, Series B **20**(1) (1958), 102–107.

8. E. T. Lee and J. W. Wang, *Statistical Methods for Survival Data Analysis*, 3rd ed., John Wiley & Sons, New York, 2003.

9. B. Efron, *Logistic regression, survival analysis, and the Kaplan–Meier curve*, Journal of the American Statistical Association **83** (1988), 414–425.

10. S. R. Jammalamadaka and A. Sengupta, *Topics in Circular Statistics*, World Scientific, Singapore, 2001.

11. M. R. Leadbetter, G. Lindgren, and H. Rootzén, *Extremes and Related Properties of Random Sequences and Processes*, Springer, Berlin, 2012.

12. B. Meriem, A. M. Gemeay, E. M. Almetwally, Z. Halim, E. Alshawarbeh, A. T. Abdulrahman, and E. Hussam, *The Power XLindley distribution: statistical inference, fuzzy reliability, and COVID-19 application*, Journal of Function Spaces **2022** (2022), Article ID 9094078.

13. S. Nedjar and H. Zeghdoudi, *On gamma Lindley distribution: properties and simulations*, Journal of Computational and Applied Mathematics **298** (2016), 167–174.

14. N. Saaidia, T. Belhamra, and H. Zeghdoudi, *On ZLindley distribution: statistical properties and applications*, Studies in Engineering and Exact Sciences **5** (2024), 3078–3097.

15. G. Chowell and H. Nishiura, *Transmission characteristics of Ebola virus disease outbreak in Nigeria, July–September 2014*, Eurosurveillance **20** (2015), 21041.

16. R. J. H. Dunn, K. M. Willett, P. W. Thorne, E. V. Woolley, I. Durre, A. Dai, D. E. Parker, and R. S. Vose, *HadISD: a quality-controlled global synoptic report database for selected variables at long-term stations from 1973–2011*, Climate of the Past **8** (2012), 1649–1679.

17. R. Kays, M. C. Crofoot, W. Jetz, and M. Wikelski, *Terrestrial animal tracking as an eye on life and planet*, Science **348**(6240) (2015), aaa2478.

Badreddine Boumaraf, Laboratory of Modeling and Socio-Economic Analysis in Water Science " MASESE", University of Souk Ahras, 41000, Algeria.
E-mail address: b.boumaaraf@univ-soukahras.dz

and

LaPS Laboratory, Badji Mokhtar–Annaba University, Annaba, 23000, Algeria.
E-mail address: halim.zeghdoudi@univ-annaba.dz